THE ARCHIVES OF MECHANICAL ENGINEERING

VOL. LIII 2006 Number 1

**Key words:** *piezoelectric actuators, shunt damping, finite element analysis*

*ROMAN FILIPEK* *, *JERZY WICIAK* *

# FEM ANALYSIS OF BEAM VIBRATIONS CONTROL USING PIEZOELECTRIC TRANSDUCERS AND A RLC SHUNT CIRCUIT

Structural vibration damping via piezoelectric shunt circuits has received a great deal of attention recently as they are light, easy to use and provide for good vibration damping performance. This study investigates vibration damping of a clamped-free beam under harmonic excitations in the steady state. The damping control strategy utilises the piezoelectric properties of PZT materials and a shunt circuit consisting of series RLC elements in parallel configuration. The analysis was made for the first mode frequency and, at the same time, for the four resonance frequencies.

## 1. Introduction

Rapid development of material engineering accompanied by major advances in engineering technologies gave rise to a new research area: the study of materials which, owing to their adaptive properties, can change their characteristics in variable surroundings. Adaptive behavior may involve the changes of shape, rigidity, position, natural vibrations frequency and other mechanical properties in response to variations of temperature or electromagnetic field [4], [5], [6], [10], [13], [17], [24]. Materials displaying adaptive properties are referred to as intelligent or smart materials [2], [7], [21], [25], [26].

Structural vibration damping via piezoelectric shunt circuits has received a great deal of attention recently as they are light, easy to use and provide for good vibration damping performance. There are many kinds of shunt circuits, including resistive, inductive, capacitive and switched ones [16]. The resonant shunt circuit consists of three standard components: a capacitor, a resistor and an inductor. The resistor-inductor (R-L) element connected

* *AGH University of Science and Technology, Department of Mechanics and Vibroacoustics, Al. Mickiewicza 30, 30-095 Kraków; E-mail: wiciak@agh.edu.pl*

in series or in parallel, displays the dynamic behaviour similar to that of mechanical vibration absorbers. Following the principle of a mechanical absorber, the resonant shunt must be tuned accordingly to absorb the vibration energy of the system's target mode [11], [16]. The direct piezoelectric effect is utilised whereby mechanical energy of the vibrating structure is converted into electrical energy. This converted energy can be dissipated as Joule heating through the load resistor of a shunt circuit when the electric resonant frequency matches mechanical frequencies. However, in order to maximize the energy dissipation at the resonance frequency of the system, it is required that the optimal inductance and resistance of shunt circuit be chosen [12].

Many researchers have developed theoretical backgrounds to represent the mechanism of a shunting damper. The potentials of passive piezoelectric damping application were first explored by Forward [9]. Hagood and von Flotow [11] investigated the potential of dissipating mechanical energy using passive electrical circuits and presented the general model for two shunt circuits: an individual resistor and a series RL configuration. Pota et al [20] presented resonant controllers for smart structures. In the paper [16], a cantilever beam with a pair of PZT patches was investigated to demonstrate theoretically and experimentally the single resonant shunt damping capabilities. Fleming and Moheimani [8] used a single piezoelectric patch to simultaneously damp multiple modes of a simply supported beam. Moheimani [15] presents an overview of literature on the subject of piezoelectric shunt damping techniques and discusses the recent reports on the feedback nature of piezoelectric shunt damping systems. This strategy is used in control of vibrations of a 1-dof mass through the use of a multilayer stack piezoelectric actuator coupled with impedance comprising a RL circuit [14].

A basic mechanical model to determine the electric field in the bimorph actuators and functionally graded actuators is presented in the papers [22], [23].

This study investigates vibration damping of a clamped-free beam under harmonic excitations, in the steady state. The damping control strategy utilises the piezoelectric properties of PZT materials and a shunt circuit consisting of series RLC elements in parallel configuration. The analysis was made for the first mode frequency and, at the same time, for the four resonance frequencies.The investigated problem is that of an Bernoulli-Euler beam with an ideally bonded piezoelectric element. The detailed solution is given in [19], where the investigated beam is divided in three sections. As regards the first and third section, we are faced with a classical problem. In the case of the second section, the task to be solved is that of a three-layer beam with outer layers made of PZT materials.

Experimental verification data relating to applications of piezoelectric elements in active reduction of flexural vibration of a cantilever beam are summarized in [18], [19]. This study utilizes the FEM approach in order to show the algorithm of procedures, which should be applicable to more complex geometries as well.

## 2. Tested object

The piezoelectric shunting experiment was performed on a steel beam with rectangular cross-section, clamped at one end. Transducers made of materials displaying the piezoelectric properties (PZT) are bonded on the beam's two outer surfaces, becoming an integral part of it. The surface in contact with the beam and the outer surface are metal-covered, forming two electrodes. One of them is grounded, and voltage can be preset across the other.

The beam is positioned in the xy plane and loaded with a harmonically variable force, directed along the z axis. Two cases are considered, depending on the manner the force is applied. In the first case, the concentrated force is applied to the beam axis, at the distance 110 mm from the beam support. In the latter case, the beam was loaded at its free end. In both cases the amplitude would approach 0.1 N. The geometry of the model and the points at which the concentrated force is applied (designated as F', F") are shown in Fig 1. The material properties are summarised in Table 1. Numerical computations utilise the FEM approach supported by Ansys software [1].

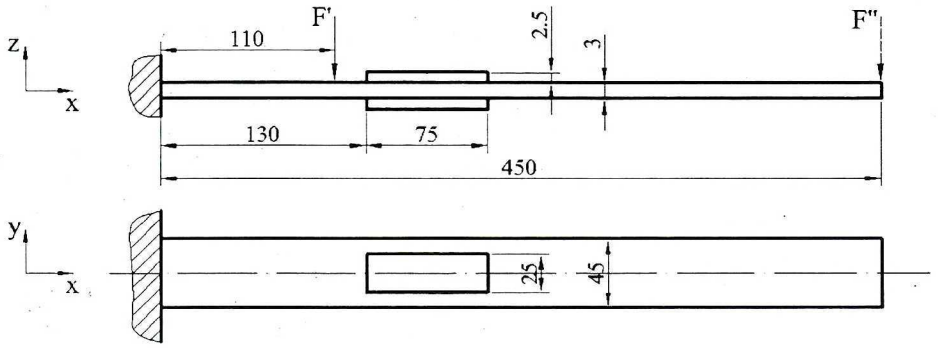


Fig. 1. Model geometry

Table 1.

Material properties of the experimental beam and transducers

| Piezoceramic PZT4 | Steel |
|---|---|
| Density 7500 $kg \cdot m^{-3}$ | Density 7700 $kg \cdot m^{-3}$ |
| Damping Ratio 0.0003 | Damping Ratio 0.0003 |
| Elasticity Modulus in X and Y direction $7.86 \cdot 10^{10}$ Pa<br>Elasticity Modulus in Z direction $6.25 \cdot 10^{10}$ Pa | Elasticity Modulus $2 \cdot 10^{11}$ Pa |
| Poisson Ratio (XY) 0.29, Poisson Ratio (XZ) 0.45 | Poisson Ratio 0.29 |
| $d_{31}$ $-1.18 \cdot 10^{-10}$, $d_{33}$ $2.73 \cdot 10^{-10}$, $d_{51}$ $4.04 \cdot 10^{-10}$ $m \cdot V^{-1}$ | |
| Permittivity in X and Y direction 804.6<br>Permittivity in Z direction 659.7 | |

The FEM analysis of beam vibration control using the piezoelectric shunt-damping approach involves several steps:

- selection of elements modelling the beam, modal analysis, harmonic analysis in the frequency range of the first four modes;
- connecting the series RL element (a resistor and an inductor connected) to piezoelectric transducers; optimisation of the shunt circuit parameters in order to reduce vibration amplitude for an individual resonance frequency;
- modelling of the shunt circuit consisting of a resistor, an inductor and a capacitor connected in series followed by optimisation of circuit parameters allowing simultaneous vibration damping for the four modes.

## 3. Modal analysis

Several elements are available in the Ansys package for the purpose of beam modelling. The element known as BEAM189 seems most advanced and based on Timoshenko's theory. However, its design precludes the addition of piezoelectric layers. As the beam thickness is relatively small in relation to its remaining parameters, the model utilises shell elements (SHELL 63, SHELL 93) which do not share this drawback. It is apparent (see table 2) that this model seems to agree well with that based on BEAM189. The elements SHELL93 have additional nodes at the edges (an 8-node element), which vastly improves the accuracy of computations while compared to SHELL63 (a 4-node element).

The option, where several layers of solid elements (SOLID186) are used, was rejected as that would increase the number of nodes and hence the calculations would take much longer.

Table 2.

Natural frequencies of cantilever beam with no piezoelectric elements

| Mode | Frequency [Hz] | | | Error [%] | |
|---|---|---|---|---|---|
| | Theoretical results | Results obtained using Ansys | | | |
| | | Element type: | | Element type: | |
| | | SHELL93 | BEAM189 | SHELL93 | BEAM189 |
| 1 | 12.20 | 12.28 | 12.20 | 0.656 | 0.000 |
| 2 | 76.47 | 76.92 | 76.42 | 0.588 | 0.065 |
| 3 | 214.15 | 215.55 | 213.90 | 0.654 | 0.117 |
| 4 | 419.65 | 423.33 | 419.03 | 0.877 | 0.148 |

Piezoelectric transducers are modelled using a 20-node coupled-field element SOLID226. A transducer comprising a single layer of elements is bonded to the beam by joint nodes whilst the adhesive layer is neglected.

The material damping ratio, independent of frequency, is taken from literature [3] as $3 \cdot 10^{-4}$ for the whole system.

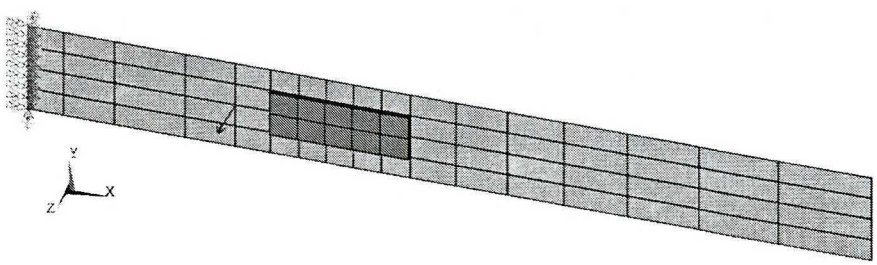


Fig. 2. FEM model of a beam with piezoelectric elements

The electromechanical constitutive equations for linear material behaviour can be written as:

$$\{T\} = [c]\{S\} - [e]\{E\} \tag{1}$$

$$\{D\} = [e]^T\{S\} - [\varepsilon]\{E\} \tag{2}$$

or alternatively:

$$\begin{Bmatrix} \{T\} \\ \{D\} \end{Bmatrix} = \begin{bmatrix} [c] & [e] \\ [e]^T & -[\varepsilon] \end{bmatrix} \begin{Bmatrix} \{S\} \\ -\{E\} \end{Bmatrix} \tag{3}$$

where: {T} – stress vector, {D} – electric flux density vector, {S} – strain vector, {E} – electric field vector, [c] – elasticity matrix, [e] – piezoelectric stress matrix, [ε] – dielectric matrix (evaluated at constant mechanical strain).

The piezoelectric stress matrix [e] may be introduced as the piezoelectric strain matrix [d]. Ansys provides for its automatic transformation utilising the elasticity matrix [c], in accordance with the formula:

$$[e] = [c][d] \tag{4}$$

On introducing the relationships given in [1] (Chapter 2. Piezoelectrics) and applying the finite element discretization, the coupled finite element matrix equation derived for a one element model becomes:

$$\begin{bmatrix} [M] & [0] \\ [0] & [0] \end{bmatrix} \begin{Bmatrix} \{\ddot{u}\} \\ \{\ddot{V}\} \end{Bmatrix} + \begin{bmatrix} [C] & [0] \\ [0] & [0] \end{bmatrix} \begin{Bmatrix} \{\dot{u}\} \\ \{\dot{V}\} \end{Bmatrix} + \begin{bmatrix} [K] & [K^Z] \\ [K^Z]^T & [K^d] \end{bmatrix} \begin{Bmatrix} \{u\} \\ \{V\} \end{Bmatrix} = \begin{Bmatrix} \{F\} \\ \{L\} \end{Bmatrix} \tag{5}$$

where [M] is structural mass matrix, [C] – damping matrix, [K] – structural stiffness matrix, $[K^d]$ – dielectric conductivity matrix, $[K^Z]$ – piezoelectric coupling matrix, {F} – structural load vector (nodal forces, surface forces, and body forces), {L} – electrical load vector (nodal, surface, and body charge), u – vector of nodal displacements, V – vector of nodal electrical potential.

The elements CIRCU94 were applied in simulations of an electric circuit, revealing five linear circuit components: a resistor, an inductor, a capacitor, a current source and a voltage source. The finite element equations for resistor, inductor, capacitor and the current source of CIRCU94 are derived from the nodal analysis method that enforces the Kirchhoff's current law at each circuit node. In order to ensure compatibility with the system of FEM equations for piezoelectric elements, the nodal analysis method is adapted accordingly to maintain the charge balance at each node.

## 4. Passive vibration control

The passive piezoelectric shunting techniques utilise piezoelectric transducers which absorb the mechanical energy of the system. These transducers are bonded to the vibrating structure and connected to an electric impedance $Z_e$. Piezoelectric shunting is accomplished by connecting a series circuit comprising a resistor R and an inductor L to the transducer terminals (Fig. 3). The adding of the PZT, an electrically capacitive element, forms a resonant circuit (resistor, inductor, capacitor) tuned to the resonance frequency of the composite structure through the control of inductance $L_i$. In order to control i-th mode, $L_i$ is derived from the formula:

$$L_i = \frac{1}{\omega_i^2 C_p} \tag{6}$$

where:

$C_p$ – capacitance of piezoelectric transducers at constant strain

$\omega_i$ – electrical resonant frequency.

The resistance R is chosen such that the overall generated electric energy be dissipated (converted into heat). Like in dynamic mechanical dampers, low circuit damping yields good resonance control though vibrations might be even enhanced in the near-resonance region.

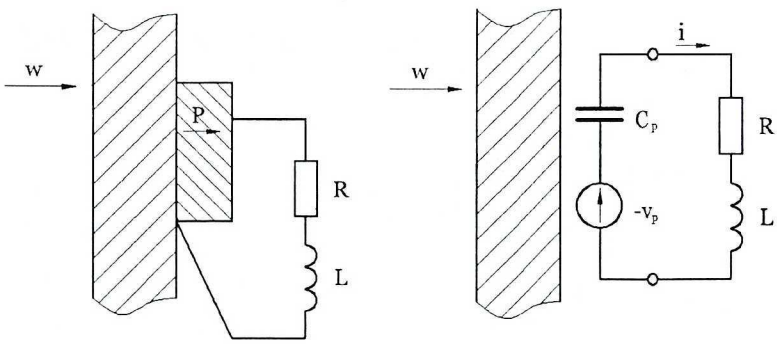


Fig. 3. Piezoelectric transducer with a series RL element and an equivalent electric circuit where w represent the external disturbance, P – electric field, $v_p$ – voltage induced inside transducer, i – current

Shunt damping approaches fall in two broad categories: single- and multiple-mode shunting. Single mode techniques are simple, though they allow only one structural mode to be damped for every PZT. Multiple-mode shunt damping techniques require more complicated shunt circuits but are capable of handling several modes. Piezoelectric patches are bonded to the structure. The equivalent electric circuit of the PZT element in the single-mode shunt damping experiment is shown in Fig. 4a, comprises the impedance $Z_m$ element governing the vibrating beam, the impedance $Z_p$ element describing the piezoelectric transducer and the impedance of an electric circuit $Z_e$. The impedance element $Z_e$ might be extended [8], [15] to the form $Z_e'$ shown in Fig. 4b which would allow multiple mode damping.

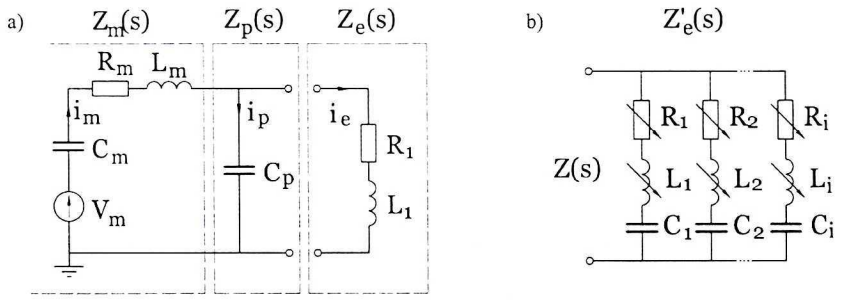


Fig. 4. a – Equivalent electric circuit of piezoelectric elements in the single mode shunt damping, b – Electric impedance used in simultaneous damping of several structural modes

## 5. Numerical analysis of vibration damping for a individual resonance frequency

The parameter R of the electric circuit for the first mode damping might be chosen by two methods. One method, proposed by Hagood and von Flotow [11], utilises a tuning criterion whereby the peak amplitude of the system transfer function be minimised. Alternatively, an optimisation method is available in the Ansys package.

A. HAGOOD AND VON FLOTOW'S ANALYTICAL METHOD

The analytical procedure involves several steps. First, the generalised electromechanical transverse coupling coefficient $K_{31}$ for the bonded piezoelectric is derived based on the frequency change of the electric boundary conditions:

$$K_{31} = \sqrt{(\omega_o^2 - \omega_s^2)/\omega_s^2} \tag{7}$$

$\omega_o$ and $\omega_s$ are the PZT open-circuit and short-circuit modal frequencies for the cantilever beam (determined experimentally or numerically).

The optimal circuit damping is expressed as:

$$r_{opt} = \sqrt{2} \cdot K_{31}/(1 + K_{31}^2) \tag{8}$$

whilst the dissipation tuning parameter is related to R by:

$$r = RC_p\omega_o \tag{9}$$

Accordingly, combining equations (3) and (4), the optimal series shunt resistance becomes:

$$R_{opt1} = \frac{r_{opt}}{C_p\omega_o} \tag{10}$$

B. OPTIMISATION METHOD (ANSYS)

The optimisation of dissipation tuning parameter r utilises the tools available in the package Ansys. The resistance R is taken as the design variable.

The cost function is assumed whereby the maximal displacements on the beam end at near- resonance frequencies be minimised.

$$J = \{uz_{max}(f_i, R_k) : |f_i - f_r| < \Delta f_r, k = 1, ..., N\} \tag{11}$$

where: $uz_{max}$ – maximal displacement on the beam end in the direction of z-axis, $R_k$ – resistance value in the subsequent iteration, $f_r$ – resonance frequency.

The Subproblem Approximation Method was applied in the optimisation. This is an advanced method supported by approximation (curve fitting) for all dependent variables (state variables and the objective (cost) function). The method is based on approximations of the objective function and state variables and is capable of converting the constrained optimisation problems to unconstrained ones. Accordingly, the relationship between the objective function and the design variables is established through curve fitting. This is accomplished by computing the objective function values for several sets of design variables, followed by the least squares fit procedure. The resulting curve is referred to as an "approximation". Each iteration generates a new data point and the objective function approximation is updated accordingly. This approximation is then minimised instead of the actual objective function. In this case a quadratic plus cross term fit is used.

C. VIBRATION DAMPING FOR THE FIRST RESONANT FREQUENCY

The optimisation method required that the capacitance of the piezoelectric transducer and inductance be first determined.

The piezoelectric transducer capacitance was obtained basing on the static analysis of the model under input excitations from voltage V applied to the transducer electrode. Given the charge Q accumulated on the electrode, the capacitance is derived from the formula:

$$C_p = \frac{Q}{V} \tag{12}$$

Equation (6) yields the inductance level required to tune the electric circuit to the resonant frequency of the system.

Applying the formulas (7–10) yields resistance $R_{opt1} = 97490\Omega$ for $C_p = 6.6532 \cdot 10^{-9}$ F, $L_1 = 23833$ H. That was followed by the optimisation of damping in the electric circuit. The subsequent steps in the optimisation procedure are shown in Fig. 5. The optimal resistance for the assumed parameters was found to be $R_{opt2} = 84839\ \Omega$. The relationship between the amplitude

of displacements along the z-axis and frequency at various resistance levels is shown in Fig. 6.

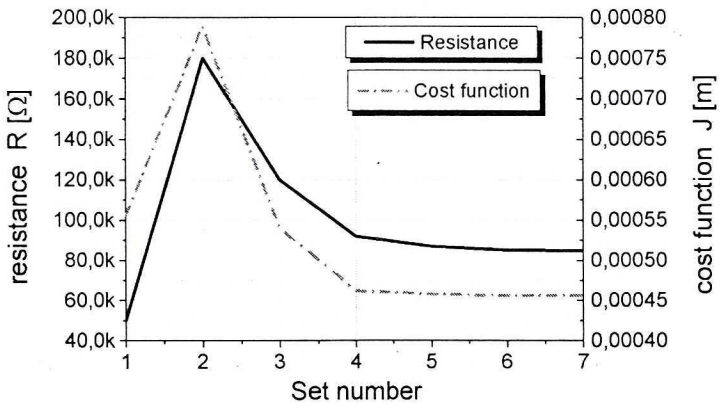


Fig. 5. Optimisation procedure: Resistance values chosen in each iteration and cost function in each iteration step

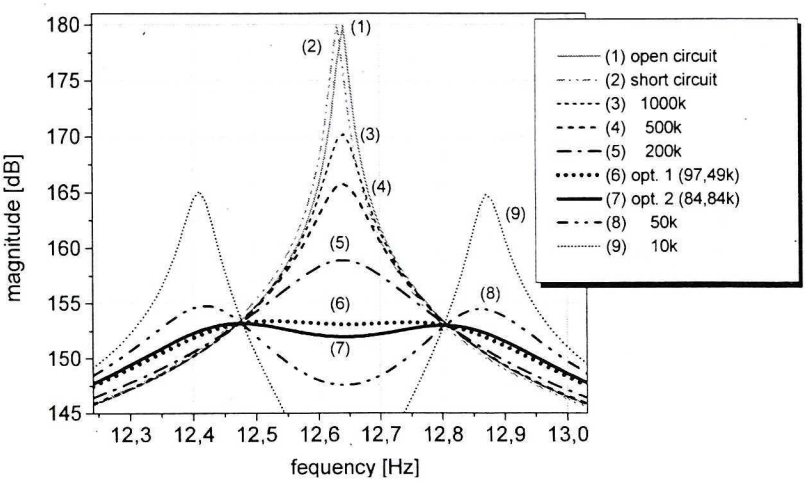


Fig. 6. Displacement amplitude along the z-axis on the beam end vs frequency for variable resistance R

The procedure would yield the optimal resistance $R_{opt2}$ at which the maximal displacement on the beam end would amount to 0.456 mm. In relation to displacements registered when the electric circuit was switched off (10.12 mm), the response reduction was achieved up to 26.9 dB. Simulation data for the two types of excitations are summarised in Table 3.

Table 3.

Compiled simulation results

| | First point of excitation | | Second point of excitation | |
|---|---|---|---|---|
| | Undamped | Damped | Undamped | Damped |
| Displacements $u_z$ [m] | 0.010119 | 0.000456 | 0.097388 | 0.004468 |
| Displacements level $L_{uz}$ [dB] | 180.1 | 153.2 | 199.8 | 173.0 |
| Damping level [dB] | 26.9 | | 26.8 | |
| Sensor voltage [V] | 132.51 | 6.38 | 1275.28 | 63.46 |
| Shunt voltage [V] | | 120.07 | | 1133.51 |

Furthermore, the system performance was tested under the other input excitations. The registered displacements were correspondingly 4.47 mm and 97.39 mm, and the response reduction was observed up to 26.8 dB. In real life conditions displacements of the order of 0.1 m would actually destroy the beam yet in the accepted model they are regarded as linear. The maximal electric field strength value (300 V/mm) is taken from the manufacturer's specifications for a material displaying similar physical parameters. Hence the admissible voltage difference across the piezoelectric transducer electrodes is taken as 750 V. Under the other type of excitations the voltages exceed the safe levels.

## 6. Numerical analysis of several modes damping

Four structural modes can be damped simultaneously using one sensor-actuator couple and four parallel combinations of resonant mode controllers with blocking capacitors with the capacitance $C_i$. Electric circuit parameters for individual circuit branches were first derived from (6) and by the method outlined in the previous subsection. Taking into account the blocking capacitors, the equivalent capacitance of an individual branch is given as:

$$C_{eqi} = \frac{1}{C_p} + \frac{1}{C_i} \tag{13}$$

These parameters being found for the first four resonant frequencies, computed inductances $L_1,\ldots,L_4$ had to be further tuned using the subproblem optimisation method, because of strong interactions with the remaining circuit branches.

The objective function was formulated as the difference between the corresponding resonant frequencies of the electric circuit $f_{ie}$ for predetermined inductances and resonant frequencies of the mechanical system $f_{im}$.

The optimisation procedure would involve the minimisation of the objective function expressed as:

$$J = \left[ \sum_{i=1}^{n} \frac{|f_{ie} - f_{im}|}{f_{im}} \right] \tag{14}$$

The additional resistance fitting $R_1, \ldots, R_4$ would proceed in a similar manner.

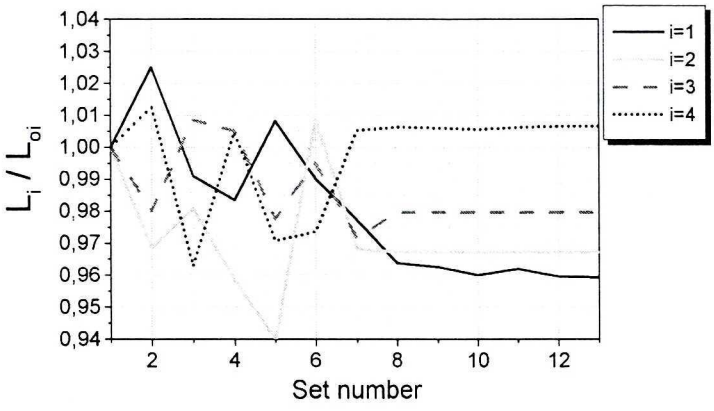


Fig. 7. Simultaneous optimisation of inductance values (ratio of forecasted $L_i$ value to the initial value $L_{oi}$ in each iteration)

Parameters of branches of the electric circuit are compiled in Table 4 for the first and second type of applied excitations. Frequency responses of these systems are shown in Fig. 8–11. Maximal displacements at the beam end, the damping ratios and voltages across the piezoelectric transducer electrodes are compiled in Table 5.

Table 4.

Parameters of circuit branches for both cases of applied excitations

| mode | f [Hz] | L [H] | R [Ω] | C [F] |
|---|---|---|---|---|
| 1 | 12.639 | 175000 | 159700 | $1 \cdot 10^{-9}$ |
| 2 | 73.795 | 5180 | 38200 | $1 \cdot 10^{-9}$ |
| 3 | 211.98 | 635.2 | 16200 | $1 \cdot 10^{-9}$ |
| 4 | 418.69 | 167.4 | 2395.3 | $1 \cdot 10^{-9}$ |

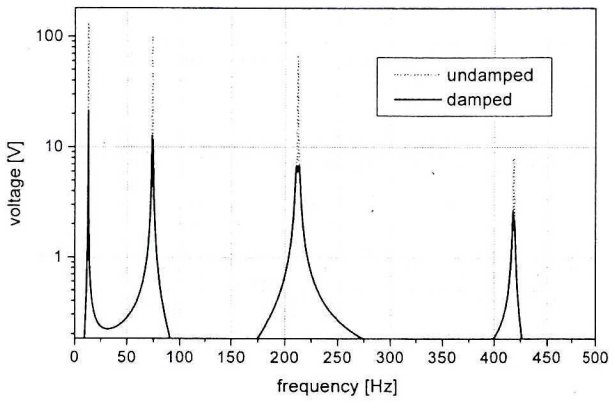


Fig. 8. Voltage vs excitation frequency for the on- state and off-state controller

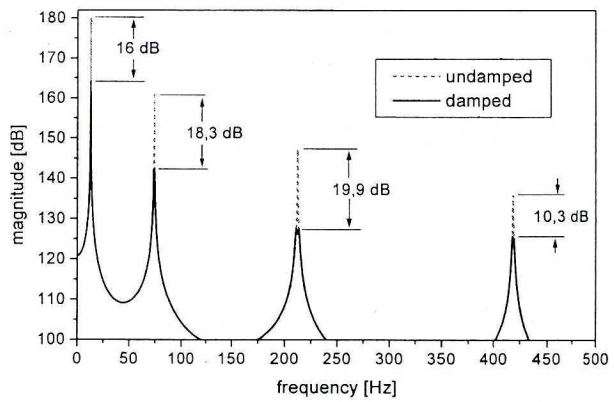


Fig. 9. Displacement on the beam end vs excitation frequency for the on-state and off-state controller

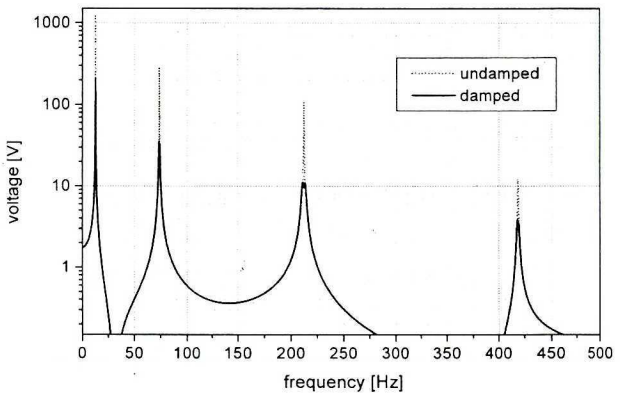


Fig. 10. Voltage across the sensor with the on-state and off-state control system

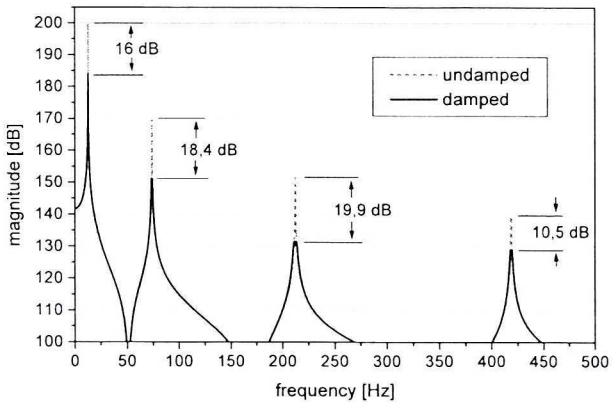


Fig. 11. Displacement on the beam end along the z-axis with the on-state and off-state control system

Table 5.

Compiled simulation results

| First point of excitation | | | | | | | | |
|---|---|---|---|---|---|---|---|---|
| Mode | Undamped | | Damped | | Damping level [dB] | Sensor voltage [V] | | Shunt voltage [V] |
| | Displacements uz [m] | Displacements level $L_{uz}$ [dB] | Displacements uz [m] | Displacements level $L_{uz}$ [dB] | | Undamped | Damped | |
| 1 | 0.010119 | 180.1 | 0.001600 | 164.1 | 16.0 | 132.51 | 21.32 | 110.28 |
| 2 | 0.001085 | 160.7 | 0.000132 | 142.4 | 18.3 | 102.21 | 12.65 | 54.81 |
| 3 | 0.000232 | 147.3 | 0.000023 | 127.4 | 19.9 | 68.00 | 6.85 | 32.58 |
| 4 | 0.000063 | 135.9 | 0.000019 | 125.6 | 10.3 | 8.00 | 2.63 | 57.10 |
| Second point of excitation | | | | | | | | |
| Mode | Undamped | | Damped | | Damping level [dB] | Sensor voltage [V] | | Shunt voltage [V] |
| | Displacements uz [m] | Displacements level $L_{uz}$ [dB] | Displacements uz [m] | Displacements level $L_{uz}$ [dB] | | Undamped | Damped | |
| 1 | 0.097388 | 199.8 | 0.015471 | 183.8 | 16.0 | 1275.28 | 206.91 | 1054.50 |
| 2 | 0.003042 | 169.7 | 0.000366 | 151.3 | 18.4 | 286.46 | 35.12 | 154.65 |
| 3 | 0.000372 | 151.4 | 0.000038 | 131.5 | 19.9 | 108.94 | 11.12 | 51.73 |
| 4 | 0.000095 | 139.5 | 0.000028 | 129.0 | 10.5 | 12.10 | 3.82 | 86.83 |

## 7. Conclusions

The modelling of the flexural actuation of the cantilever beam and modelling of a tuned electrical absorber is investigated. The numerical analysis proved the adequacy of a single actuator and proposed resonant controllers in single and multi-modal control of smart beams. The performance of finely tuned piezoelectric shunt damping systems is sensitive to resonance frequencies of the system.

In the case of vibration damping for an individual resonant frequency. the response reduction was observed up to 27 dB for the first mode for the two types of applied excitations. In the case of multiple mode damping the respective response reductions were: 16 dB, 18 dB, 20 dB and 10 dB for the first, second, third and fourth resonant frequency. The reduction of vibration power would bring about the decrease of voltage generated across the sensor. Accordingly, a 6-fold voltage reduction was observed.

Such amplitude reduction is possible for the comparable beam thickness (3 mm) and piezoelectric elements (2.5 mm each). Furthermore, the assumption of an ideally elastic bonding of PZT elements seems a major simplification. In a more accurate model and in analytical methods there is an added layer of glue, of finite thickness. The distance between the beam axis and the surface of a piezoelectric layer is neglected, which might affect the final result. This omission is associated with the use of shell elements.

Application of series RLC elements connected in parallel while handling several modes adversely impacts on the vibration reduction performance for the individual frequency while compared to a single RL circuit.

In real experimental model, the first resonance frequency has to be omitted when the excitation applied comes from forces at the beam end. Alternatively, the amplitude of the exciting signal has to be reduced, since during simulations the circuit parameters tend to exceed the admissible levels, which might lead to beam damage or voltage breakdown across piezoelectric elements.

These controllers can be effectively used in other applications for example in active control of acoustic noise.

This study is a part of the research project 4T07B 03429 supported by the Ministry of Science and Information Society Technologies.

Manuscript received by Editorial Board, June 15, 2005;
final version, November 28, 2005.

## REFERENCES


[1] Ansys user manual v. 9.0, 2004.

[2] Craig A. R: Intelligent Material Systems-The Dawn of a New Materials Age. Center for Intelligent Material Systems and Structures. Virginia Polytechnic Institute and State University, 1992.

[3] Cremer L., Heckl M., Ungar E. E.: Structure-Borne Sound, Springer Verlag, 1988.

[4] Cupial P.: Three-Dimensional Natural Vibration Analysis of Piezoelectric Rectangular Plates. Proceedings of the Eight International Congress on Sound and Vibration. Ho18dB. 20. Hong Kong, 2001, pp. 1925÷1932.

[5] Cupiał P.: Some Analytical and Finite Element solutions of the Vibration of Piezoelectric Continua. XX Symposium: Vibrations in Physical systems. Poznań-Blażejewko, 2002.

[6] Elliott S., Gardonio P., Vibroacoustics (1): Active structural acoustic control. NATO Advanced Course: Responsive Systems for Active Vibrations Control. Brussels, 2001.

[7] Elliott S. P., Nelson P. A.: Active Control of Vibrations. Academic Press. London, 1997.

[8] Flaming A. J., Moheimani S. O. R.: Adaptive piezoelectric shunt damping. Smart Materials and Structures 12 (2003), pp. 36÷48.

[9] Forward R.L.: Electronic damping of vibrations in optical structures. J. of Applied Optics. 18(5), 1979, pp. 690÷697.

[10] Fuller C. R.: Active Control of Sound Transmission/ Radiation From Elastic Plates by Vibration Inputs: I Analysis. J. of Sound and Vibration (1990), 136(1), pp. 1÷15.

[11] Hagood N. H., von Flotow A.: Damping of Structural Vibrations With Piezoelectric Materials and Passive Electrical Network. J. of Sound and Vibration (1991), 146 (2), pp. 243÷268.

[12] Kim J., Kim J-H.: Multimode shunt damping of piezoelectric smart panel for noise reduction. Journal of the Acoustical Society of America. 116 (2) 2004, pp. 942÷948.

[13] Kozień M. S., Wiciak J.: Acoustics Radiation of a Plate With Line and Cross Type Piezoelectric Elements. Molecular and Quantum Acoustics. vol. 24, 2003, pp. 97÷108.

[14] Krzyżyński T., Oleśkiewicz R.: Modelling and simulation of impedance shunt branches in passive vibration damping with piezo-elements. XI Warsztaty Naukowe Polskiego Towarzystwa Symulacji Komputerowej „Symulacja w badaniach i rozwoju" (red. T. Krzyżyński, A. Tylikowski), 2004, pp. 38÷45.

[15] Moheimani S. O. R.: A Surwey of Recent Innovations in Vibration Damping and Control Using Shunted Piezoelectric Transducers. IEEE Transactions on Control System Technology, V.11, No. 4, 2003, pp. 482÷494.

[16] Park C. H.: Dynamics modelling of beams with shunted piezoelectric elements. Journal of Sound and Vibration 268, (2003), pp. 115÷129.

[17] Pietrzakowski M.: Composites with Piezoceramic Fibers and Integrated Electrodes in Vibration Control. Mechanika, t. 22, z. 3, 2003, pp. 375.

[18] Pietrzakowski M.: Experimental verification of use of piezoelectric elements in active reduction of flexural vibration. XI Warsztaty Naukowe Polskiego Towarzystwa Symulacji Komputerowej „Symulacja w badaniach i rozwoju" (red. T. Krzyżyński, A. Tylikowski), 2004, pp. 46÷51.

[19] Pietrzakowski M.: Active Damping of Transverse Vibration Using Distributed Piezoelectric Elements. Prace Naukowe Politechniki Warszawskiej, 2004.

[20] Pota H. R, Moheimani S. O. R., Smith M.: Resonant controllers for Smart Structures. Smart Materials and Structures 11 (2002), pp. 1÷8.

[21] Tylikowski A.: Aktywne tłumienie w elementach ciągłych konstrukcji i maszyn. w: Tłumienie drgań. red. J. Osiński. PWN. Warszawa, 1997.

[22] Tylikowski A.: Symulacyjne badania aktuatorów wykonanych z piezoelektrycznych materiałów gradientowych VIII Warsztaty Naukowe Polskiego Towarzystwa Symulacji Komput-

erowej „Symulacja w badaniach i rozwoju" (red. T. Krzyżyński, A. Tylikowski), 2001, pp. 384÷388.

[23] Tylikowski A.: The influence of electrical and Electromechanical Properties of Functionally Graded Piezoelectric Actuators. XI Warsztaty Naukowe Polskiego Towarzystwa Symulacji Komputerowej „Symulacja w badaniach i rozwoju" (red. T. Krzyżyński, A. Tylikowski), 2004, pp. 14÷21.

[24] Waanders J. W.: Piezoelectric ceramics. Properties and applications. Philips Components. Eindhoven, 1991.

[25] Wada B. K., Fanson J. L., Crawley E. F.: Adaptive Structures. B. Wada. editor. Adaptive Structures. pp. 1÷8. New York. 1989. ASME.

[26] Wang Z., Chen S. C., Han W.: The static shape control for intelligent structures. Finite Elements in Analysis and Design 26 (1997), pp. 303÷314.

**Analiza sterowania drganiami belki za pomocą przetworników piezoelektrycznych i obwodu elektrycznego RLC przy wykorzystaniu MES**

Streszczenie

W ostatnich latach zauważa się wzrost zastosowania przetworników piezoelektrycznych wraz z obwodami elektrycznymi RLC, ze względu na właściwości elektromechaniczne, do tłumienia drgań strukturalnych.

W pracy przedstawiono analizę tłumienia drgań belki jednostronnie utwierdzonej przy wymuszeniu harmonicznym, w stanie ustalonym. Tłumienie drgań uzyskano poprzez zastosowanie elementów piezoelektrycznych typu PZT i obwodu elektrycznego złożonego z równolegle połączonych dwójników szeregowych RLC. Analizę sterowania drganiami przeprowadzono dla pierwszej częstotliwości drgań oraz dla jednocześnie dla czterech pierwszych częstotliwości rezonansowych.